

# Dark Matter Candidates in a Visible Heavy QCD Axion Model

Hajime Fukuda,<sup>1,\*</sup> Masahiro Ibe,<sup>1,2,†</sup> and Tsutomu T. Yanagida<sup>1,‡</sup>

<sup>1</sup>*Kavli IPMU (WPI), UTIAS, The University of Tokyo, Kashiwa, Chiba 277-8583, Japan*

<sup>2</sup>*ICRR, The University of Tokyo, Kashiwa, Chiba 277-8582, Japan*

(Dated: August 13, 2018)

## Abstract

In this paper, we discuss dark matter candidates in a visible heavy QCD axion model. There, a mirror copied sector of the Standard Model with mass scales larger than the Standard Model is introduced. By larger mass scales of the mirrored sector, the QCD axion is made heavy via the axial anomaly in the mirrored sector without spoiling the Peccei-Quinn mechanism to solve the strong  $CP$ -problem. Since the mirror copied sector possesses the same symmetry structure with the Standard Model sector, the model predicts multiple stable particles. As we will show, the mirrored charged pion and the mirrored electron can be viable candidates for dark matter. They serve as self-interacting dark matter with a long range force. We also show that the mirrored neutron can be lighter than the mirrored proton in a certain parameter region. There, the mirrored neutron can also be a viable dark matter candidate when its mass is around 100 TeV. It is also shown that the mirrored neutrino can also be a viable candidate for dark matter.

---

\* e-mail: hajime.fukuda@ipmu.jp

† e-mail: ibe@icrr.u-tokyo.ac.jp

‡ e-mail: tsutomu.tyanagida@ipmu.jp

## I. INTRODUCTION

The Peccei-Quinn (PQ) mechanism [1–4] is the most successful solution to the strong  $CP$ -problem. There, the PQ-symmetry is assumed to be almost exact which is broken only by the axial anomaly of QCD. After its spontaneous breaking, the associated pseudo Nambu-Goldstone boson, the axion  $a$ , obtains a non-vanishing potential by non-perturbative effects of QCD through the axial anomaly. Eventually, the effective  $\theta$ -angle is dynamically tuned to be vanishing by the vacuum expectation value (VEV) of the axion.

For a successful PQ-mechanism, however, it is required to circumvent a lot of constraints put by extensive axion searches [5, for review]. The most popular approach to evade those constraints is to make the axion couple to the Standard Model particles very feeble, so that the axion is invisible [6–9]. There, the decay constant of axion,  $f_a$  (and hence the PQ-breaking scale), is taken to be very large, *e.g.*,  $f_a > 10^9$  GeV.

Another approach to evade the constraints is to make the axion heavy (see *e.g.* [10, 11] for early attempts). Among various attempts, a successful idea was proposed in [12] where a mirror copy of the Standard Model was introduced. By larger mass scales of the mirrored sector, the QCD axion is made heavy via the axial anomaly in the mirrored sector without spoiling the PQ solution to the strong  $CP$ -problem. This idea has been incarnated by a model constructed in [13] in which experimental, astrophysical and cosmological constraints are examined carefully (see also [14–17] for relevant discussions). Resultantly, it has been shown that the axion decay constant can be as low as  $f_a \simeq \mathcal{O}(1)$  TeV when the axion mass is rather heavy,  $M_a > \mathcal{O}(0.1)$  GeV. We call this model a visible heavy axion model.

One of the advantage of the heavy axion model with a moderate decay constant is that the model is durable against explicit breaking of the PQ symmetry by Planck suppressed operators which are generically expected in quantum gravity [18–23]. For example, the shift in the effective  $\theta$  angle is as small as of  $\mathcal{O}(10^{-11})$  even in the presence of dimension five PQ-breaking operator for  $f_a \simeq \mathcal{O}(1)$  TeV and  $M_a = \mathcal{O}(1)$  GeV.<sup>1</sup>

In this paper, we discuss dark matter candidates in the visible heavy QCD axion model. In [13], it has been deferred to discuss whether the mirrored sector provides good candidates for dark matter. In fact, the model predicts multiple stable particles since the mirror copied sector possesses the same symmetry structure with the Standard Model sector. They are

---

<sup>1</sup> See discussions in the appendix A.

the photon ( $\gamma'$ ), the nucleons ( $N'$ ), and two of the electron ( $e'$ ), the lightest neutrino ( $\nu'$ ) and the charged pion ( $\pi'^{\pm}$ ) in the mirrored sector. Therefore, it is enticing to ask whether they can be good candidates for dark matter.

As we will show,  $\pi'^{\pm}$  with masses in the TeV range can be a viable candidate for dark matter when it is lighter than all of  $\nu'$ . It is also shown that  $e'^{\pm}$  with a mass in the hundred GeV range can also be a viable candidate. Notably,  $\pi'^{\pm}$  and  $e'^{\pm}$  serve as self-interacting dark matter with a long range force. It should be noted that such darkly-charged dark matter is severely constrained [24–26]. Recently, however, it has been pointed out that there are a number of mitigating factors to the constraints, which revives possibility of darkly-charged dark matter [27]. We also show that the mirrored neutron,  $n'$ , can be lighter than the mirrored proton,  $p'$ , and hence, be the lightest baryon in the mirrored sector. Accordingly, it can also be a viable dark matter candidate when its mass is around 100 TeV. It is also shown that  $\nu'$  also can be a viable candidate for dark matter.

The paper is organized as follows. In section II, we briefly review the visible heavy axion model in [13]. In section III, we discuss the dark matter candidates in the mirrored sector of the visible heavy axion model. The final section is devoted to our conclusions and discussions.

## II. MODEL OF VISIBLE HEAVY QCD AXION

In this section, we first review a model of visible heavy QCD axion [13]. In this model, a copy of the standard model is introduced following the Rubakov's idea [12]. There, we assume a  $\mathbb{Z}_2$  exchanging symmetry between the Standard Model and its mirror copy. Due to the  $\mathbb{Z}_2$  symmetry, the  $\theta$ -angles in these two sectors are aligned at the high energy input scale, *i.e.*  $\theta = \theta'$ . Throughout this paper, objects in the copied sector are referred with a prime ( $'$ ).

To implement the PQ mechanism, we introduce QCD colored left-handed Weyl fermions,  $\psi_L$  and  $\bar{\psi}_R$ , and those for QCD',  $\psi'_L$  and  $\bar{\psi}'_R$ . We choose the PQ charges of  $\psi_L$  and  $\psi'_L$  to be 0 and the ones of  $\bar{\psi}_R$  and  $\bar{\psi}'_R$  to be  $-1$ . A complex scalar  $\phi$  with a PQ charge  $+1$  is introduced to break the PQ-symmetry spontaneously. As in the KSVZ axion model [6, 7],

$\phi$  couples to  $\psi$  and  $\psi'$  via

$$\Delta\mathcal{L} = g\phi\psi_L\bar{\psi}_R + g\phi\psi'_L\bar{\psi}'_R + \text{H.c.}, \quad (1)$$

where  $g$  is a coupling constant. Here, we assume that  $\phi$  is even under the  $\mathbb{Z}_2$  symmetry.

Assuming that  $\phi$  obtains a VEV, we decompose  $\phi$  into an axion  $a$  and a scalar boson  $s$ ,

$$\phi = \frac{1}{\sqrt{2}}(f_a + s)e^{ia/f_a}. \quad (2)$$

Here,  $f_a$  is the decay constant of the axion. Due to the VEV of  $\phi$ ,  $\psi$ 's become heavy vector-like quarks with masses

$$m_\psi^{(\prime)} = \frac{g}{\sqrt{2}}f_a. \quad (3)$$

We additionally introduce small mixings between  $d_i^{(\prime)}$  ( $i = 1, 2, 3$ ) quarks in the Standard Model<sup>( $\prime$ )</sup> and  $\psi^{(\prime)}$  by assuming appropriate gauge charges,

$$\Delta\mathcal{L} = \varepsilon_i\mu\psi_L\bar{d}_{Ri} + \varepsilon_i\mu\psi'_L\bar{d}'_{Ri}, \quad (4)$$

where  $\varepsilon_i \ll 1$  are small mixing parameter and the  $\mu$  is a representative mass scale of  $\mathcal{O}(m_\psi)$ . Through the mixing term,  $\psi$ 's decay into Standard Model and corresponding mirror sector quarks.<sup>2</sup>

It should be emphasized that the axion is common among the Standard Model and its mirrored copy. With a single axion, the effective  $\theta$  angles of QCD and QCD' are simultaneously set to be zero due to the  $\mathbb{Z}_2$  symmetry. Since  $\theta$  and  $\theta'$  hardly run under the renormalization group evolution [28], they are aligned even below the spontaneous breakdown of the  $\mathbb{Z}_2$  symmetry. Because of the breaking, the dynamical scale of QCD' can become much higher than that of QCD (see [13] for details). With a large dynamical scale of QCD', the axion obtains the mass dominantly from QCD',

$$M_a^2 \simeq \frac{m'_u m'_d}{(m'_u + m'_d)^2} \frac{m_\pi'^2 f_\pi'^2}{f_a^2}, \quad (5)$$

where  $m'_{u,d}$  are the masses of  $u'$  and  $d'$  quarks,  $m'_\pi$  the mass of  $\pi'$ ,  $f'_\pi$  the decay constant of

---

<sup>2</sup> We may instead assume mixings between  $u^{(\prime)}$  quarks and  $\psi^{(\prime)}$ .

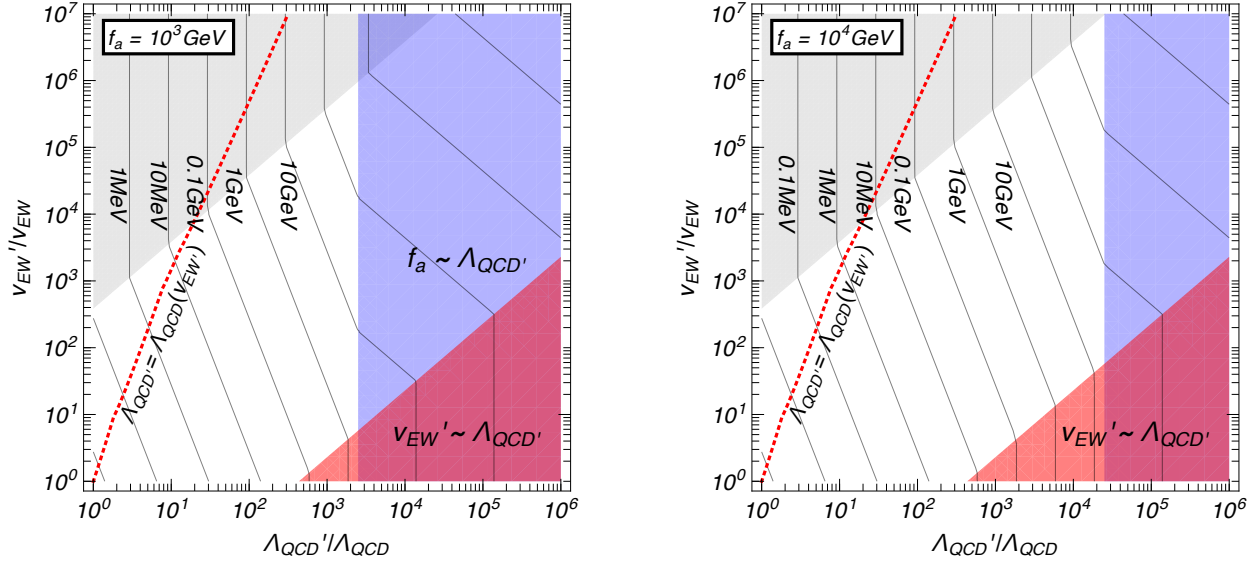


FIG. 1. Contour plots of the axion mass as a function of  $\Lambda'_{\text{QCD}}$  and  $v'_{\text{EW}}$  for given  $f_a$ . Here, we take  $f_\pi \simeq 93 \text{ MeV}$ ,  $m'_{u,d}/m'_d \simeq m_u/m_d = 0.56$ ,  $\Lambda_{\text{QCD}} \simeq 400 \text{ MeV}$  and  $v_{\text{EW}} \simeq 174 \text{ GeV}$ . In the gray shaded regions, the quark masses in the mirrored sector are larger than  $\Lambda'_{\text{QCD}}$  where the axion mass does not depend on the quark mass any more. In the blue shaded regions, the PQ-symmetry breaking is caused by the condensation of  $\psi'_L \bar{\psi}'_R$  due to the strong dynamics and hence  $f_a = \mathcal{O}(\Lambda'_{\text{QCD}})$ . In the red shaded regions, the electroweak symmetry breaking and the VEV of Higgs' in the mirrored sector is caused by the condensations of quarks', leading to  $v'_{\text{EW}} \simeq \mathcal{O}(\Lambda'_{\text{QCD}})$ .

$\pi'$ . In terms of the dynamical scale of QCD' and the VEV of Higgs',  $v'_{\text{EW}}$ , those quantities are given by

$$m'_{u,d} \simeq m_{u,d} \times \frac{v'_{\text{EW}}}{v_{\text{EW}}}, \quad m_{\pi'} \simeq m_\pi \times \frac{\Lambda'_{\text{QCD}} v'_{\text{EW}}}{\Lambda_{\text{QCD}} v_{\text{EW}}}, \quad f'_\pi \simeq f_\pi \times \frac{\Lambda'_{\text{QCD}}}{\Lambda_{\text{QCD}}}. \quad (6)$$

In the following analysis, we assume that the  $\mathbb{Z}_2$  exchanging symmetry is softly (or spontaneously) broken and take  $\Lambda'_{\text{QCD}}$  and  $v'_{\text{EW}}$  are independent parameters (see [13] for concrete examples). Note that if  $\Lambda'_{\text{QCD}}$  is greater than the tree-level Higgs' VEV, the electroweak symmetry is broken by  $\Lambda'_{\text{QCD}}$  and  $v'_{\text{EW}} \sim \Lambda'_{\text{QCD}}$  is induced.

In Fig. 1, we show contour plots of the axion mass as a function of  $\Lambda'_{\text{QCD}}$  and  $v'_{\text{EW}}$  for given  $f_a$ . Here, we take  $f_\pi \simeq 93 \text{ MeV}$ ,  $m'_{u,d}/m'_d \simeq m_u/m_d = 0.56$ ,  $\Lambda_{\text{QCD}} \simeq 400 \text{ MeV}$  and  $v_{\text{EW}} \simeq 174 \text{ GeV}$ . In the gray shaded regions, the quark masses in the mirrored sector are larger than  $\Lambda'_{\text{QCD}}$  where the axion mass does not depend on the quark mass any more.<sup>3</sup> We call this region as the heavy quark region. In the blue shaded regions, the PQ-symmetry

<sup>3</sup> In the figure, the boundary between these two regimes is taken to  $m'_\pi$  in Eq. (6) is equal to  $m'_u + m'_d$ .

breaking is caused by the condensation of  $\psi'_L \bar{\psi}'_R$  due to the strong dynamics and hence  $f_a = \mathcal{O}(\Lambda'_{\text{QCD}})$ . In the red shaded regions, the electroweak symmetry breaking in the mirrored sector is caused by the condensations of quarks', leading to  $v'_{\text{EW}} \simeq \mathcal{O}(\Lambda'_{\text{QCD}})$  as mentioned above. In the figure, we also show the parameter region where  $\Lambda'_{\text{QCD}}$  is increased purely by the effects of larger quark masses in the mirrored sector due to a large  $v'_{\text{EW}}$  (red dashed lines).<sup>4</sup>

As discussed in [13], the mirrored sector is in thermal equilibrium with the Standard Model sector in the early universe, via the axion exchange. As the temperature of the universe decreases and becomes much lower than the axion mass, the mirrored sector decouples from the Standard Model sector. Thus, when the axion is much heavier than the QCD phase transition temperature,  $T_{\text{QCD}} = \mathcal{O}(100) \text{ MeV}$ , the contributions of the copied sector to the effective number of relativistic species are sufficiently suppressed due to  $\Lambda'_{\text{QCD}} \gg \Lambda_{\text{QCD}}$ . For a lighter axion, on the other hand,  $\gamma'$  decouples below  $T_{\text{QCD}}$  and contributes the dark radiation, which causes tensions with the Big-Bang Nucleosynthesis and the Cosmic Microwave Background (CMB). To avoid such problems, we concentrate on parameter regions where  $M_a \gtrsim 1 \text{ GeV}$  in the following arguments.<sup>5</sup>

Let us also summarize the constraints and the visibility of the heavy axion model at collider experiments. For a rather heavy axion,  $M_a \gtrsim 3m_\pi$ , the constraints from the beam dump experiments such as the CHARM experiment [30] are not applicable due to its short lifetime. The axion in this mass range is also free from the constraints from the rare  $K$ -meson decay [31] since the axion mode is closed. The constraints from the rare  $B$ -meson decays are also evaded due to the lack of the direct axion couplings to the quarks as in the case of the KSVZ axion model.

The LHC experiments put lower limits on the mass of the extra quarks  $\psi$ . The experimental lower limits on the extra quark masses are 800–900 GeV [32–35], depending on the branching ratios of  $\psi$  into  $b$  and  $t$  quarks. Assuming  $g \sim 1$ , the current constraints require  $f_a \gtrsim 1 \text{ TeV}$ .

The radial and the axion components of  $\phi$  (*i.e.*  $s$  and  $a$ ) can be also produced at the LHC experiments via the couplings to the gluons, when their masses are below a TeV range. For example, the production cross sections of  $s$  would be  $\mathcal{O}(100\text{--}1) \text{ fb} \times (1 \text{ TeV}/f_a)^2$  for

<sup>4</sup> The effects of  $\psi'$  contributions to the renormalization group running of the coupling constant of QCD' do not cause visible difference in the figures even for  $\Lambda'_{\text{QCD}} \gg m'_\psi$ .

<sup>5</sup> As discussed in [29], the coupling between the axion and  $\gamma'$  may be suppressed. In that case, the constraints on the axion mass come only from the following experiments.

$M_s \simeq 500 \text{ GeV} - 1 \text{ TeV}$ , which mainly decays into a pair of the axions. The majority of axions subsequently decay into a pair of jets for  $M_a \gg \mathcal{O}(100) \text{ MeV}$ . A part of them decay into  $2\gamma$ , whose branching ratio is  $\alpha^2/\alpha_s^2 \sim 0.01$  or more [29]. Since  $s$  is much heavier than  $a$ , the final decay products of each axion are highly collimated and look like a single jet and photon, respectively. Comparing the branching ratio with the background, this one photon plus one jet channel may be most sensitive to search  $s$ . For example, if we simply scale the current backgrounds at ATLAS 13 TeV search [36], we can conclude that it is possible to detect  $s$  for the integrated luminosity  $3 \text{ ab}^{-1}$  in some parameter region. Once such an excess is observed, we can study the difference between a single photon and collimated photons [37]. Note that if  $a$ - $\gamma'$ - $\gamma'$  coupling is suppressed, as is mentioned above, the axion may be as light as  $3m_\pi \sim 400 \text{ MeV}$ . In that region, the branching ratios of  $a \rightarrow 2\gamma$  and  $a \rightarrow \text{mesons}$  are comparable and diphoton like channel may be most sensitive [29].

### III. DARK MATTER CANDIDATES IN THE MIRRORED SECTOR

#### A. Stable Particles

Stable particles in the mirrored sector are  $\gamma'$ ,  $N'$ , and two of  $\nu'$ ,  $e'$  and  $\pi'^{\pm}$ . In the minimal model of the visible heavy axion model, each the Standard Model and the mirrored sector has a single Higgs doublet, and hence,  $U(1)_{\text{QED}}$  and  $U(1)'_{\text{QED}}$  are not broken spontaneously. Thus,  $\gamma'$  is massless and stable. The stabilities of other particles are associated with symmetries, *i.e.*  $B'$ ,  $L'$  and  $Q'_{\text{QED}}$  symmetries.

In the Standard Model sector, we assume the seesaw mechanism to account for the tiny neutrino masses [38, 39] [see also 40]. If the seesaw mechanism also works in the mirrored sector, the neutrino masses in the mirrored sector,  $m'_{\nu}$ , is enhanced by  $(v'_{EW}/v_{EW})^2$ , which easily exceeds the upper limit on the hot dark matter mass,  $m'_{\nu} \ll \mathcal{O}(10) \text{ eV}$ , from CMB lensing and cosmic shear [41].<sup>6</sup> To evade this constraint, we assume that the seesaw mechanism does not take place in the mirrored sector. This can be achieved by turning off spontaneous breaking of the  $B' - L'$  symmetry in the mirrored sector so that the Majorana masses of the right-handed neutrinos in the mirrored sector vanish (see [13] for details).

---

<sup>6</sup> Here, we roughly translate the constraint on the gravitino mass,  $m_{3/2} \lesssim 4.7 \text{ eV}$  (95% C.L.) [41], by assuming that the decoupling temperature of  $\nu'$  from the thermal bath of the Standard Model sector is similar to the gravitino.

When the spontaneous breaking of the  $B' - L'$  symmetry is turned off, thermal leptogenesis [42] [see 43–45, for review] does not take place in the mirrored sector. Accordingly, there is no  $B'$  asymmetry in the mirrored sector when the  $B$  asymmetry in the Standard Model sector is provided by thermal leptogenesis. This feature is important for the  $N'$  relic density not to exceed the observed dark matter density even for  $m'_N \gg 1 \text{ GeV}$ .

In this set up,  $\nu'$ s obtain the Dirac neutrino masses via the Yukawa interaction to the Higgs boson. Depending on the Yukawa coupling,  $\nu'$ s can be lighter or heavier than  $\pi'^{\pm}$ . When (at least one of)  $\nu'$ s are lighter than  $\pi'^{\pm}$ ,  $\pi'^{\pm}$  decays into a pair of charged lepton' and  $\nu'$ . On the other hand,  $\pi'^{\pm}$  becomes stable when all the  $\nu'$ s are heavier than  $\pi'^{\pm}$ . Therefore, the stable particles in the mirrored sector are

$$\begin{cases} \gamma', e', \pi'^{\pm}, N', & (\text{for } m'_\nu > m'_{\pi^\pm}), \\ \gamma', e', \nu', N', & (\text{for } m'_\nu < m'_{\pi^\pm}). \end{cases} \quad (7)$$

In the following, we discuss whether we have good dark matter candidates in each possibility.

Let us comment here that  $m'_\nu \ll m'_{\pi^\pm}$  can be automatically achieved if there are only two generations of the right-handed neutrinos in each sector. In fact, the lightest  $\nu$  and  $\nu'$  are both massless. It should be also noted that two generations of the right-handed neutrinos are enough for successful thermal leptogenesis in the Standard Model sector [46–49].

## B. Masses of Dark Matter Candidates

In Fig. 2, we show the masses of the stable particles. The average nucleon mass is approximately estimated by

$$m_{N'} \equiv \frac{m'_n + m'_p}{2} \simeq \left( \frac{m_n + m_p}{2} - 3\bar{m} \right) \times \frac{\Lambda'_{\text{QCD}}}{\Lambda_{\text{QCD}}} + 3\bar{m} \times \frac{v'_{EW}}{v_{EW}}, \quad (8)$$

where  $\bar{m}$  is an average of the  $u$  and  $d$  quark masses,  $m_u = 2.2_{-0.4}^{+0.6} \text{ MeV}$  and  $m_d = 4.7_{-0.4}^{+0.5} \text{ MeV}$  [50].<sup>7</sup> The  $N'$  masses are dominated by the masses of the quark' when the quark' masses are heavier than  $\Lambda'_{\text{QCD}}$ .<sup>8</sup>

<sup>7</sup> There is an  $\mathcal{O}(1)$  ambiguity for the quark' mass contributions for  $\Lambda'_{\text{QCD}} \ll \bar{m}'$ . However, the contributions from the quark' mass to  $m'_{N'}$  is only important when the quark' mass is larger than  $\Lambda'_{\text{QCD}}$ , where nucleon mass can be approximated by  $3 \times \bar{m}'$ .

<sup>8</sup> For  $v'_{EW} \gg 10^{5-6} \times v_{EW}$ ,  $m'_\psi$  can be smaller than  $m'_{u,d}$  for  $f_a \simeq 10^3 \text{ GeV}$ . In such region, the lightest baryon consists of  $\psi'$ s, and hence, the  $N'$  mass in the figure for  $v'_{EW} \gg 10^{5-6} \times v_{EW}$  should not be taken literally.



The mass difference between the neutron' ( $n'$ ) and the proton' ( $p'$ ) is estimated by

$$m_{n'} - m_{p'} \simeq \delta m_{n-p}^{\text{QED}} \times \frac{\Lambda'_{\text{QCD}}}{\Lambda_{\text{QCD}}} + \kappa_N (m_d - m_u) \times \frac{v'_{EW}}{v_{EW}}, \quad (9)$$

where  $\delta m_{n-p}^{\text{QED}}$  denotes the electromagnetic contribution to the  $n-p$  mass difference, and  $\kappa_N$  parameterizes the isospin-violating contribution. As leading order approximations, we use the central values of the Standard Model [51]

$$\delta m_{n-p}^{\text{QED}} = -0.178_{-0.064}^{+0.0004} \text{ GeV} \times \alpha_{\text{QED}}, \quad (10)$$

$$\kappa_N = 0.95_{-0.06}^{+0.08}. \quad (11)$$

Remarkably,  $n'$  can be lighter than  $p'$  when  $\Lambda'_{\text{QCD}}$  becomes very large. In fact, in the green shaded region in Fig. 2,  $p'$  is lighter than  $n'$ , while  $n'$  is lighter in the other region. It should be also noted that the mass difference is smaller than  $m'_{\pi^\pm}$  in the entire parameter region, and hence, both of  $p'$  and  $n'$  are stable for  $m'_\nu > m'_{\pi^\pm}$ . If one of the neutrino' mass and  $m'_e$  is light enough, on the other hand, the heavier  $N'$  can decay into the lighter one.

The mass of  $\pi'^0$  is estimated to be

$$m_{\pi'^0}^2 \simeq m_{\pi^0}^2 \times \frac{\Lambda'_{\text{QCD}} v'_{EW}}{\Lambda_{\text{QCD}} v_{EW}} \quad (12)$$

for  $m'_u + m'_d < m'_{\pi^0}$ . For  $m'_u, m'_d \gtrsim \Lambda'$ , It is dominated by  $m'_u + m'_d$  in the heavy quark mass region.<sup>9</sup> The mass of  $\pi'^\pm$  is, on the other hand, given by,

$$m_{\pi'^\pm}^2 \simeq m_{\pi^0}^2 + \alpha'_{\text{QED}} \Lambda_{\text{QCD}}^2, \quad (13)$$

where  $\alpha'_{\text{QED}}$  is the fine-structure constant of the QED'.

Finally, the mass of  $e'$  is given by,

$$m'_e = m_e \times \frac{v'_{EW}}{v_{EW}}. \quad (14)$$

It should be noted that the  $\mu'$  decays into  $3e'$  via box diagrams in which  $W'$  boson circulate. Thus,  $\mu'$  cannot be a candidate for dark matter.

---

<sup>9</sup> In the parameter region where  $m'_\psi$  is smaller than  $m'_{u,d}$ , the lightest meson consist of  $\psi'$ . Thus, again, the mass of the pion in the figure should not be taken literally.

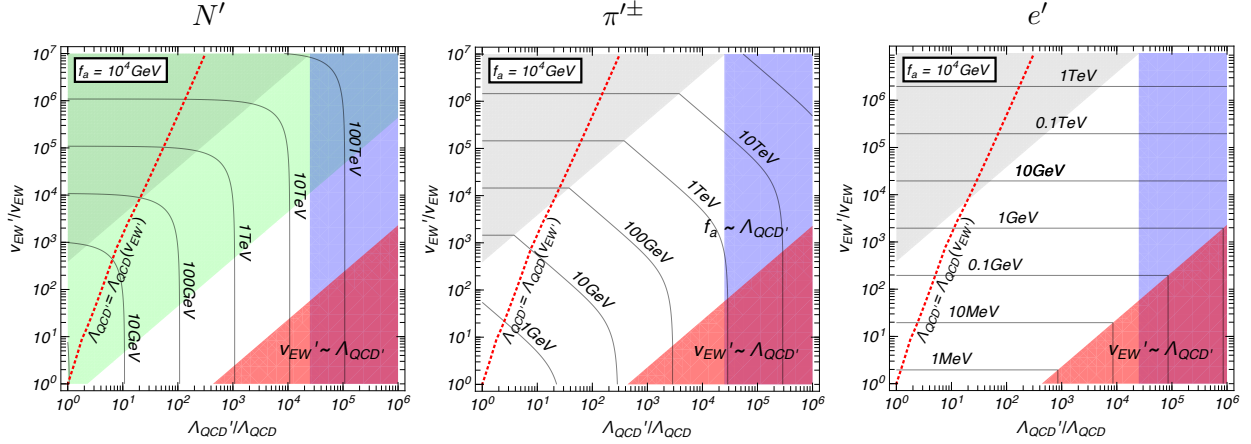


FIG. 2. Contour plots of the masses of  $N'$ ,  $\pi'^{\pm}$  and  $e'$ . The gray, blue and red shaded regions are the same with the ones in Fig. 1. The axion decay constant  $f_a$  does not affect the masses of the stable particles, which only shifts the blue shaded regions. In the green shaded region of the mass of  $N'$ ,  $p'$  is lighter than  $n'$ , while  $n'$  is lighter in the other region.

### C. Dark Matter Candidates For $m'_{\nu} > m'_{\pi^{\pm}}$

First, let us discuss dark matter candidates for  $m'_{\nu} > m_{\pi^{\pm}}$ , where  $n'$ ,  $p'$ ,  $\pi'^{\pm}$  and  $e'$  are stable. To explain the observed dark matter density,  $\Omega h^2 \simeq 0.1198 \pm 0.0015$  [52], the averaged annihilation cross section of dark matter should be of

$$\langle \sigma v \rangle \sim 3 \times 10^{-26} \text{cm}^3/\text{s}, \quad (15)$$

[53] (see also [54].) In Fig. 3, we show the annihilation cross sections of  $N'$ ,  $\pi'^{\pm}$ , and  $e'$  as functions of  $\Lambda'_{\text{QCD}}$  and  $v'_{\text{EW}}$ .

In the figure, we assume that the annihilation cross section of  $N'$  into  $\pi'$ 's saturates the so-called unitarity limit [55],

$$\langle \sigma v_{\text{rel}} \rangle \sim \frac{8\pi}{m_{N'}^2}, \quad (16)$$

where we approximate  $v_{\text{rel}}^2 \simeq 1/4$ . From the left panel of Fig. 3, we find that  $N'$  provides the observed dark matter density for  $m_{N'} \sim 100$  TeV if they are the sole dark matter candidate.

In the central panel of the figure, we show the annihilation cross section of  $\pi'^{\pm}$  into a pair of  $\gamma'$  and into a pair of  $\pi'^0$ . The averaged annihilation cross section of  $\pi'^{\pm}$  into  $\gamma'$  is given

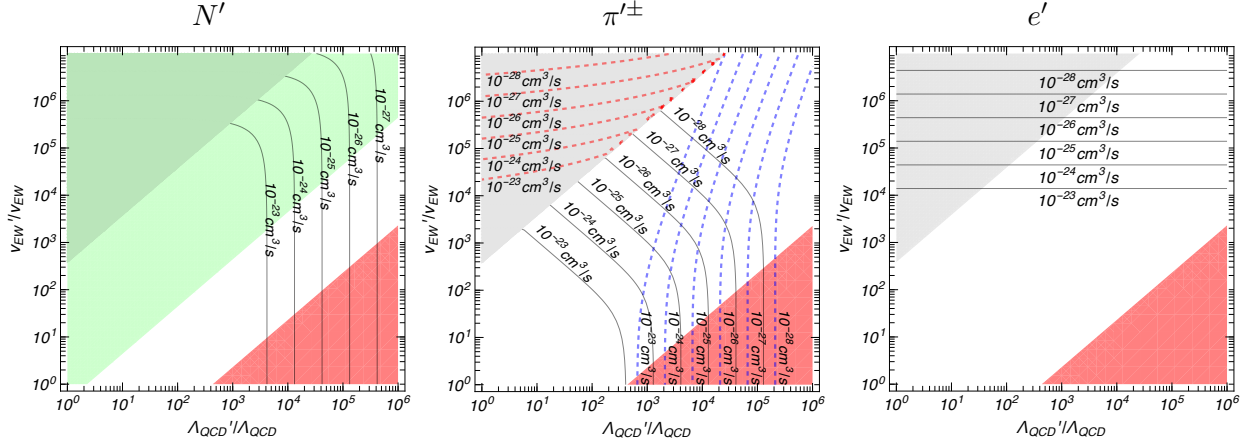


FIG. 3. Contour plots of the annihilation cross sections of  $N'$ ,  $\pi'^{\pm}$  and  $e'$ . The gray, red, and green shaded regions are the same with the ones in Fig. 2. In the left panel,  $N'$ 's annihilate into a pair of  $\pi'$ 's. In the central panel,  $\pi'^{\pm}$  annihilates into a pair of  $\gamma'$  (solid) and into a pair of  $\pi^0$  (dashed) in the region of  $m'_{\pi^{\pm}} > m'_u + m'_d$ . In the heavy quark' region, we show the annihilation cross section of  $d'$  into a pair of gluon's. In the right panel,  $e'$ 's annihilate into a pair of  $\gamma'$ 's.

by,

$$\langle\sigma v_{\text{rel}}\rangle = \frac{\pi\alpha_{\text{QED}}'^2}{m_{\pi^{\pm}}'^2}. \quad (17)$$

The annihilation cross section into  $\pi^0$  is, on the other hand, given by

$$\langle\sigma v_{\text{rel}}\rangle \simeq \frac{1}{16\pi} \frac{9}{4m_{\pi^{\pm}}'^2} \frac{m_{\pi^{\pm}}'^4}{f_{\pi}^4} \frac{(s - 4m_{\pi^0}^{\prime 2})^{1/2}}{2m_{\pi^0}'}, \quad (18)$$

where  $s \simeq 4m_{\pi^{\pm}}^{\prime 2}(1 + v_{\text{rel}}^2/4)$  (see *e.g.* [56]). In the central panel of the figure, those cross sections are shown by the solid lines and the orange dashed lines, respectively. The figure shows that the cross section of  $\mathcal{O}(10^{-26}) \text{ cm}^3/\text{s}$  is achieved for  $m'_{\pi^{\pm}} \simeq 400 \text{ GeV}$  when the mode into  $\gamma'$ 's is dominant and  $m'_{\pi^{\pm}} = \mathcal{O}(1) \text{ TeV}$  when the mode into  $\pi^0$ 's is dominant.

In the heavy quark' region, we also show the annihilation cross section of  $d'$  into gluon's,

$$\langle\sigma v_{\text{rel}}\rangle \simeq \frac{55}{216} \frac{\pi\alpha_{\text{QCD}}'^2}{m_d^{\prime 2}}. \quad (19)$$

Here, the fine structure constant of QCD' is estimated by

$$\alpha'_{\text{QCD}} \simeq \left( \frac{11}{2\pi} \log \frac{m'_d}{\Lambda'_{\text{QCD}}} \right)^{-1}. \quad (20)$$

The figure shows that the cross section of  $\mathcal{O}(10^{-26}) \text{ cm}^3/\text{s}$  is obtained for  $m'_d = \mathcal{O}(1) \text{ TeV}$ . It should be noted that the cross sections in Eqs. (18) and (19) receive large higher order corrections for  $\Lambda'_{\text{QCD}} \sim m'_u + m'_d$ , and hence, their values at  $\Lambda'_{\text{QCD}} \sim m'_u + m'_d$  are not reliable.

Finally, we also show the annihilation cross section of  $e'$  into a pair of  $\gamma'$ 's. The annihilation cross section of  $e'$  into  $\gamma'$  is given by,

$$\langle \sigma v_{\text{rel}} \rangle = \frac{\pi \alpha_{\text{QED}}'^2}{2m_e'^2}. \quad (21)$$

The cross section of  $\mathcal{O}(10^{-26}) \text{ cm}^3/\text{s}$  is achieved for  $m'_e \simeq 300 \text{ GeV}$ .

Altogether, we show the parameter region where the observed dark matter density is explained in Fig. 4 (green band). To reflect our ignorance of the precise relation between the mass parameters ( $\Lambda'_{\text{QCD}}, v'_{\text{EW}}$ ) with physical mass parameters and the interaction rates of hadron', we show the parameter region where  $\Omega h^2 = 0.03\text{--}0.3$  is achieved. As the figure shows, the observed dark matter density can be explained by  $\pi'^{\pm}$  with a mass in the TeV range for  $m'_{\pi^{\pm}} > m'_u + m'_d$  (*i.e.* the vertical brach of the green band). The dark matter density can be also explained by  $e'$  with a mass around 300 GeV for  $\Lambda'_{\text{QCD}}/\Lambda_{\text{QCD}} \simeq 10^3\text{--}10^4$  GeV on the horizontal branch of the green band. In the heavy quark' region, dark matter consists of the mixture of the quark' with a mass in the TeV range and  $e'$  with a mass around 300 GeV.<sup>10</sup> The relic density of  $N'$  is subdominant in the favored region.

It should be noted that dark matter components which annihilate into  $\pi'^0$ 's may lead the Standard Model jet via the  $a\text{--}\pi'^0$  mixing with a mixing angle of  $\mathcal{O}(f'_\pi/f_a)$ . Furthermore, the annihilation cross section is significantly enhanced when the dark matter velocity becomes small since  $\pi'^{\pm}$  couples to the massless  $\gamma'$ .<sup>11</sup> The kinetic decoupling of darkly-charged dark matter takes place at around the temperature of the Standard Model sector to be,

$$T_{\text{kd}} \sim 0.5 \text{ keV} \times \xi^{-7/3} \left( \frac{m_{DM}}{100 \text{ GeV}} \right)^{5/3}, \quad (22)$$

for  $\alpha'_{\text{QED}} \simeq 1/137$ . Here,  $\xi$  denotes the ratio between the temperatures of the mirrored sector and the Standard Model sector,

$$\xi \equiv \frac{T_{\text{mirror}}}{T} = \left( \frac{g_{*S}^{\text{mirror}}(T_D)}{g_{*S}^{\text{mirror}}(\xi T_{\text{kd}})} \right)^{1/3} \left( \frac{g_{*S}(T_{\text{kd}})}{g_{*S}(T_D)} \right)^{1/3}, \quad (23)$$

<sup>10</sup> The quark' eventually confined into charged mesons. Here, we assume that the QCD' dynamics which takes place after the dark matter freeze-out does not affect the quark' number density significantly (see *e.g.* discussions in [57, 58]).

<sup>11</sup> For enhanced annihilation rate via the bound state formation, see [25, 59–62]

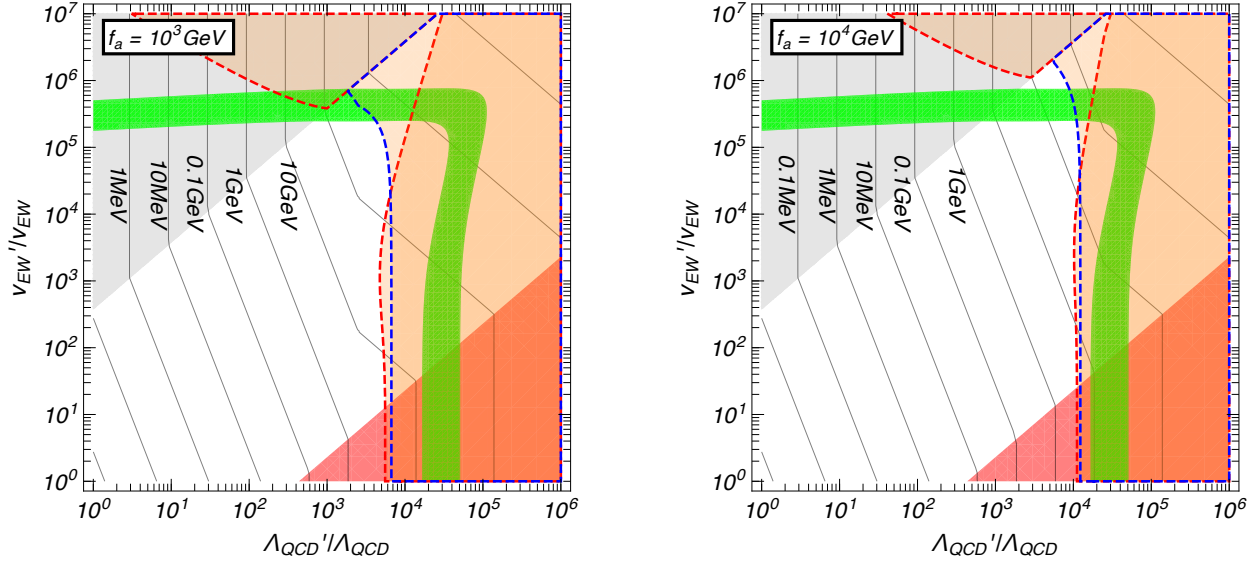


FIG. 4. The parameter region where the observed dark matter density is explained (green band) for given  $f_a$  for  $m'_\nu > m'_{\pi^\pm}$ . There, the dominant components of the dark matter are  $\pi'^\pm$ ,  $e'$  and  $e'$  and  $\pi'^\pm$  for the vertical, curved and horizontal regions, respectively. The contour plot of the axion mass is also shown. The gray shaded regions are the same with the ones in Fig. 1. The areas enclosed by the red and blue dashed lines are excluded by the constraints on the dark matter annihilation from CMB observations. The green band is not affected by  $f_a$ , while the CMB constraints get stringent for a smaller  $f_a$ .

with  $g_{*S}$  and  $g_{*S}^{\text{mirror}}$  being the degrees of freedom of the Standard Model sector and the mirrored sector, respectively. Thus, for example, the dark matter velocity at around the recombination time of the Standard Model sector is given by,

$$v_{\text{DM}} \sim 10^{-7} \times \xi^{1/6} \left( \frac{100 \text{ GeV}}{m_{\text{DM}}} \right), \quad (24)$$

with which the cross section is enhanced by the Sommerfeld enhancement factor,

$$S \simeq \frac{\pi \alpha'_{\text{QED}}/v_{\text{DM}}}{1 - e^{-\pi \alpha'_{\text{QED}}/v_{\text{DM}}}}. \quad (25)$$

It should be noted that the dark matter annihilation rate at around the recombination time is significantly constrained from CMB observations [63–72];

$$\frac{1}{2} \langle \sigma v_{\text{rel}} \rangle \lesssim 4 \times 10^{-25} \text{ cm}^3/\text{s} \times \left( \frac{0.1}{f_{\text{eff}}} \right) \left( \frac{m_{\text{DM}}}{100 \text{ GeV}} \right), \quad (26)$$

at 95%C.L. [73]. Here, we use the efficiency factor  $f_{\text{eff}} \simeq 0.1$  which is the half of the one

for the dark matter annihilation into a pair of gluons [69]. In Fig. 4, we show the parameter regions which are excluded by the CMB constraints on the annihilation cross section at around the recombination time. Here, we scale the constraint in Eq. (26) by a factor of  $(\Omega h^2/0.12)^2$  for each dark matter component. The region enclosed by the red and blue dashed lines are excluded by the annihilation rate of  $\pi'^{\pm}$  and  $p'$  into the axion, respectively. Here, we assume  $\alpha'_{\text{QED}} \simeq \alpha_{\text{QED}}$ . The figure shows that the vertical branches of the green band where  $\pi^{\pm}$  is the dominant dark matter component are excluded by the CMB observations. It should be noted that  $e'$  does not annihilate into the axion, and hence, the  $e'$  component is not constrained by the CMB observations.

The dominant component of the dark matter discussed in this section are all charged under QED', and hence, are self-interacting through a long-range force. Such darkly-charged dark matter is severely constrained by the ellipticities of galaxy and cluster-scale dark matter halos, since the long-range interactions erase the non-sphericity [24–26]. Among various constraints, the non-zero ellipticity of the gravitational potential of NGC720 [74] puts stringent constraints on the self-interaction cross section and excludes the darkly-charged dark matter with  $\alpha'_{\text{QED}} \simeq 1/137$  for  $m_{DM} \lesssim \mathcal{O}(1)$  TeV [25]. Recently, however, it is pointed out that there are some uncertainties on the ellipticity of the inner parts of the galaxy and in the estimation of the timescale to erase ellipticity, which revives the darkly-charged dark matter for  $m_{DM} = \mathcal{O}(100)$  GeV and  $\alpha'_{\text{QED}} = 1/137$  [27]. It is also pointed out that there are a number of mitigating factors as for the constraints on the darkly-charged dark matter from the dwarf galaxy survival probability [75], with which darkly-charged dark matter for  $m_{DM} = \mathcal{O}(100)$  GeV and  $\alpha'_{\text{QED}} \simeq 1/137$  is consistent.

Darkly-charged dark matter of  $m_{DM} = \mathcal{O}(0.1\text{--}1)$  TeV also has a huge self-interacting cross section per the dark matter mass of  $\mathcal{O}(10^2\text{--}10^4)$  cm<sup>3</sup>/s/g in dwarf galaxies for  $\alpha'_{\text{QED}} \simeq 1/137$  [27]. Such a large cross section affects the dark halo dynamics and could lead to core formation in dark halo [76]. However, the effects of the huge self-interacting cross section per the dark matter mass of  $\mathcal{O}(10^2\text{--}10^4)$  cm<sup>3</sup>/s/g require more detailed analysis as well as a larger statistical samples as noted in [27]. In view of these circumstances, we regard that darkly-charged dark matter candidates in this model are not ruled out currently and expect that future observations might be able to probe intriguing features of the darkly-charged dark matter as self-interacting dark matter.

#### D. Dark Matter Candidates In the Presence of a Very Light $\nu'$

Let us discuss next dark matter candidates when the lightest  $\nu'$  is very light and stable. Here, we require  $m_{\nu'} \ll \mathcal{O}(10)$  eV, so that  $\nu'$  evades the constraint from CMB lensing and cosmic shear [41]. As mentioned earlier, such a light  $\nu'$  can be automatically achieved if there are only two generations of the right-handed neutrinos in each sector, with which the lightest  $\nu^{(\prime)}$  is massless in each sector.

In this case,  $\pi^{\prime\pm}$  decays into  $\nu'$ , and hence,  $\pi^{\prime\pm}$  is no more dark matter candidate. Besides, the mass difference between  $p'$  and  $n'$  is larger than  $m'_e$  in most parameter region, and hence,  $n'$  decays into  $p'$  for  $m'_n > m'_p$  (i.e. in the green shaded region in Fig. 2) while  $p'$  decays into  $n'$  for  $m'_n < m'_p$ . In the heavy quark' mass region, on the other hand, the lightest and stable baryon corresponds to  $\Delta^{\prime++}(u'u'u')$  baryon.<sup>12</sup> As a result, the dark matter candidates in the presence of a very light (or massless)  $\nu'$  are

$$\begin{cases} e' , n' , & (m'_p > m'_n + m'_e) , \\ e' , p' , & (m'_n > m'_p + m'_e) , \\ e' , \Delta^{\prime++} , & (\text{in the heavy quark' region}) . \end{cases} \quad (27)$$

It should be noted that the very light (or massless)  $\nu'$  does not give a visible contribution to the the effective number of relativistic species,  $N_{\text{eff}}$ , as long as  $T_D \gg T_{\text{QCD}}$ . In fact,  $N_{\text{eff}}$  deviates from the Standard Model prediction,  $N_{\text{eff}}^{\text{SM}} = 3.046$  [77] by

$$\Delta N_{\text{eff}} = \left( 2 \left( \frac{11}{4} \right)^{4/3} + \frac{7}{8} \times 4 \right) \left( \frac{2}{g_{*S}(T_D)} \right)^{4/3} \times \left( \frac{7}{4} \left( \frac{4}{11} \right)^{4/3} \right)^{-1} \simeq 0.18 , \quad (28)$$

which is consistent with the  $N_{\text{eff}}$  obtained from the CMB observation,  $N_{\text{eff}} = 3.15 \pm 0.23$  (68 %C.L.).

In Fig. 5, we show that parameter where the observed dark matter density is explained. Here, we use the annihilation cross sections given in the previous section and we again allow the predicted dark matter density within  $\Omega h^2 = 0.03\text{--}0.3$ . In this case, the observed dark matter density can be explained by  $N'$  with  $m'_N \simeq 100$  TeV. In the heavy quark' region, dark matter consists of  $\Delta^{\prime++}$  with a mass in the TeV range and  $e'$  with a mass around 300 GeV.<sup>13</sup>

<sup>12</sup> Here, we assume that  $\psi'$  mixes with  $d'$  as in Eq. (4) and  $\psi'$  is heavier than  $u'$  and  $d'$ , so that both  $d'$  and  $\psi'$  decay.

<sup>13</sup> Here, the resultant number density of  $\Delta^{\prime++}$  after confinement is similar to that of  $u'$ .

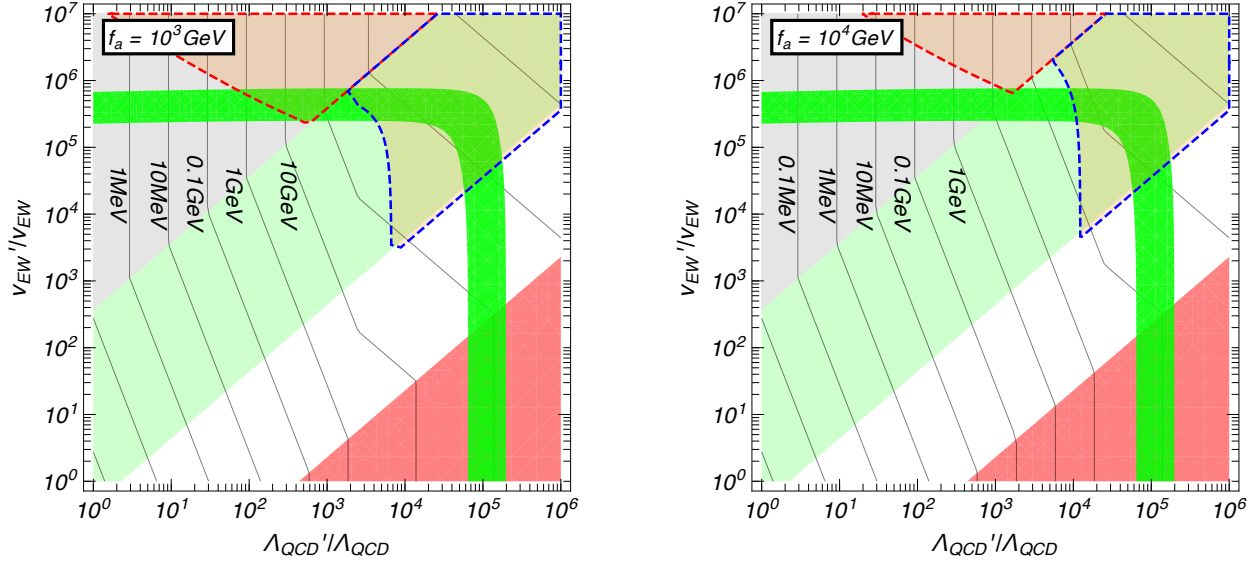


FIG. 5. The parameter region where the observed dark matter density is explained (green band) for given  $f_a$  in the presence of a very light  $\nu'$ . There, the dominant components of the dark matter are  $n'$ ,  $e'$  and  $e'$  and  $\Delta'^{++}$  for the vertical, curved and horizontal regions, respectively. The contour plot of the axion mass is also shown. The gray, blue, red and green shaded regions are the same with the ones in Fig. 1. The areas enclosed by the red and blue dashed lines are excluded by the constraints on the dark matter annihilation from CMB observations.

As a notable difference from the case with  $m'_{\nu} > m'_{\pi\pm}$ , there is a parameter region where dark matter mainly consists of neutral particle  $n'$  while  $p'$  decays away. Since  $n'$  does not couple to a long range force, this parameter region is free from the CMB constraints on the annihilation cross section at around the recombination time as well as other constraints on the self-interactions of dark matter.

Before closing this section, let us comment that the CMB constraints on the annihilation cross section at around the recombination time as well as other constraints on the self-interactions of dark matter can be easily evaded if  $U(1)'_{\text{QED}}$  is spontaneously broken and  $\gamma'$  obtains a finite mass. Such spontaneous breaking is easily achieved when each sector has two Higgs doublets. There, the  $U(1)'_{\text{QED}}$  can be broken with appropriate couplings between the two Higgs doublets in the two sectors. In this case, entire regions on the green band in Fig. 5 are viable to explain the observed dark matter density with no long-range interactions.<sup>14</sup>

<sup>14</sup> Here, we assume that  $m'_{\gamma} < m'_e$  so that  $e'$  can annihilate into  $\gamma'$ . It is also noted that  $\pi'^{\pm}$  decays into a pair of massive  $\gamma'$ 's.



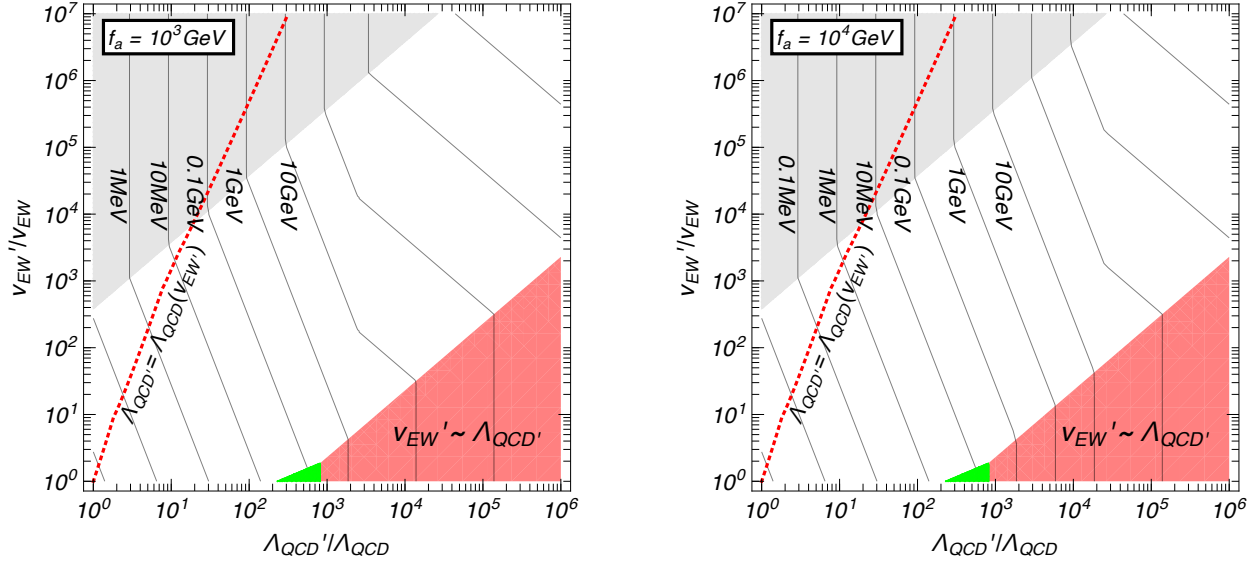


FIG. 6. The parameter region where the observed dark matter density is explained by  $\nu'$  annihilating into leptons via  $s$ -channel  $Z'$  boson. In the green shaded region, the condition,  $m'_\nu < m'_{\pi^\pm}$  is satisfied, and hence,  $\nu'$  is stable.

### E. $\nu'$ Dark Matter

As a final possibility, let us consider that Dirac  $\nu'$  dark matter which is possible for  $m'_\nu < m'_{\pi^\pm}$ . The annihilation cross section of  $\nu'$  into a pair of  $e'$ ,  $\mu'$  and  $\tau'$  via  $Z'$  exchange is given by [78]

$$\langle \sigma v_{\text{rel}} \rangle \simeq \frac{3m'_\nu{}^2}{16\pi \cos^4 \theta'_W v'^4_{EW}} \left( \left( \frac{1}{2} - \sin^2 \theta'_W \right)^2 + \left( \frac{1}{2} \right)^2 \right), \quad (29)$$

where  $\theta'_W$  is the weak mixing angle in the mirrored sector. Thus, the appropriate  $\nu'$  dark matter density is obtained when the Dirac neutrino mass satisfies

$$m'_\nu = y'_\nu v'_{EW} \simeq 8 \text{ GeV} \times \left( \frac{v'_{EW}}{v_{EW}} \right)^2. \quad (30)$$

Here,  $y'_\nu$  denotes the neutrino Yukawa coupling in the mirrored sector, and we assume  $\theta'_W \simeq \theta_W$  in the final expression.

In Fig.6, we show the parameter space which satisfies Eq.(30) and  $m'_\nu < m'_{\pi^\pm}$ . The figure shows that only a small portion of the parameter space is allowed. As the figure shows, the corresponding axion mass is lighter than 100 MeV range for  $f_a = 10^4 \text{ GeV}$  which

are excluded by the beam dump experiments and cosmological arguments [13]. The axion mass for  $f_a = 10^3$  GeV is also close to the exclusion limits though not ruled out.

So far, we have assumed that the  $B - L$  symmetry and the  $B' - L'$  symmetry are global symmetries or at most discrete gauge symmetries which are not associated with gauge bosons. If we consider that they are continuous gauge symmetries, on the other hand,  $B' - L'$  gauge boson in the mirrored sector is massless, and hence,  $\nu'$ s can annihilate into  $B' - L'$  gauge bosons with an annihilation cross section,

$$\langle \sigma v_{\text{rel}} \rangle = \frac{\pi \alpha_{B-L}'^2}{2m_{\nu'}^2} . \quad (31)$$

With this cross section, the dark matter density is explained for

$$m_{\nu'}' \simeq 400 \text{ GeV} \times \left( \frac{\alpha_{B-L}'^2}{10^{-2}} \right) , \quad (32)$$

which can be consistent with  $m_{\nu'}' < m_{\pi^\pm}'$  in large parameter region. Furthermore, by allowing slight spontaneous breaking, the constraints on the Sommerfeld enhanced annihilation as well as other constraints on the self-interactions of dark matter can be evaded.

#### IV. CONCLUSIONS AND DISCUSSIONS

In this paper, we discussed dark matter candidates in the visible heavy QCD axion model. As we have shown,  $\pi'^{\pm}$  and  $e'^{\pm}$  can be a viable candidate for dark matter when it is lighter than all of  $\nu'$  for  $f_a = 10^3$ – $10^4$  GeV. As an interesting feature, they serve as self-interacting dark matter with a long range force. We also showed  $n'$  can be also a viable dark matter candidate when its mass is around 100 TeV with one of  $\nu'$  being very light or massless. It is also shown that  $\nu'$  can also be a viable candidate for dark matter. In particular, we find that  $\nu'$  can be viable candidate in a large parameter region when the  $B' - L'$  gauge interaction is invoked.

For a moderate value of the decay constant,  $f_a \lesssim 10^4$  GeV, the model can be tested at future collider experiments via the direct production of  $s$ ,  $a$ , and the extra quarks required for the PQ-mechanism. Besides, the darkly-charged dark matter candidates annihilating into  $\pi'^0$  leave imprints on the spectrum the CMB anisotropy through the  $a$ – $\pi'^0$  mixing (see Fig. 4). The future CMB observations such as PIXIE [79] LiteBird [80], and CORE+ [81] will be

able to improve the limit on the annihilation cross section at around the recombination time. The darkly-charged dark matter candidates can also be strengthened if future observations of dark halo structure reveal that dark matter should have a long-range force.

Another dark matter candidate,  $n'$  in the hundreds TeV range, also annihilates into the axion through the  $a$ - $\pi^0$  mixing. By assuming the total annihilation cross section in Eq.(15), the annihilation cross section into the axion is of  $\mathcal{O}(10^{-28})\text{cm}^3/\text{s}$ . Such a cross section is much lower than the current constraints from the antiproton to proton ratio in the cosmic ray [82, 83] measured by AMS-02 [84].<sup>15</sup> It is also lower than the constraints from the continuous gamma ray spectrum from the dwarf spheroidal galaxies measured by Fermi-LAT [85].

Finally, let us consider the ‘‘nucleon’ decay’’ as an intriguing probe of the  $n'$  dark matter candidate in the hundreds TeV range. Since the  $B$  and  $B'$  symmetries are global symmetries, they are expected to be broken at least by Planck suppressed operators as generically expected in quantum gravity. Thus, through the Planck suppressed dimension six operators for example, the decay rate of  $n'$  into  $\nu'$  and  $\pi^0$  is roughly given by

$$\Gamma(n' \rightarrow \nu' + \pi^0) \sim \frac{1}{32\pi} \frac{m_{N'}^5}{M_{\text{PL}}^4}, \quad (33)$$

where  $M_{\text{PL}} \simeq 2.4 \times 10^{18} \text{ GeV}$  is the reduced Planck scale.<sup>16</sup> A fraction of  $n'$  decays also into axion through the  $a$ - $\pi^0$  mixing of  $\mathcal{O}(f'_\pi/f_a)$ , which subsequently decays into the QCD jets. Altogether, the lifetime of  $n'$  divided by the branching ratio into the axion is roughly given by,

$$\tau(n' \rightarrow \nu' + a) \sim 10^{28} \text{ s} \times \left( \frac{100 \text{ TeV}}{m_{N'}} \right)^5 \left( \frac{f_a}{100 \text{ TeV}} \right)^2 \left( \frac{10 \text{ TeV}}{f'_\pi} \right)^2. \quad (34)$$

The decay of dark matter into QCD jets is constrained from the observations of the extragalactic gamma-ray background (EGRB) [86–89]. The constraint on the lifetime of  $n'$  decaying into QCD jet can be read from [89]

$$\tau(n' \rightarrow \nu' + a) \gtrsim 10^{28} \text{ s} \times \left( \frac{\Omega_{n'}}{\Omega_{DM}} \right). \quad (35)$$

<sup>15</sup> Here, we roughly translate the constraints in [82, 83] for the dark matter model annihilating into  $b\bar{b}$  and  $W^+W^-$  for  $M_a \gtrsim \mathcal{O}(1) \text{ GeV}$ . For a lighter axion, it does not lead to anti-proton signals, and hence, the constraints are much weaker.

<sup>16</sup> For a rough estimation, we neglect uncertainties in hadronic matrix elements.

Notably, the constraint from the EGRB observations is close to the lifetime (divided by the branching ratio into the axion) in Eq. (34) for  $\Omega_{n'} = \Omega_{DM}$ . Therefore, the EGRB observations are indirectly probing the global symmetry breaking expected in quantum gravity through the  $n'$  decay in the mirrored sector.

Furthermore,  $n'$  dark matter can also be tested by the proton decay searches in the Standard Model sector if the Grand Unified Theory (GUT) exists at a scale  $M_{\text{GUT}}$  lower than the Planck scale. Under the assumption of the GUT, two sectors are expected to have the same GUT scale,  $M_{\text{GUT}}$ , due to the  $\mathbb{Z}_2$  exchanging symmetry. Therefore, the  $n'$  lifetime divided by the branching ratio into the axion is roughly interrelated to the proton lifetime  $\tau_p$  in the Standard Model sector,

$$\tau_p(p \rightarrow e + \pi^0) \simeq 10^{35} \text{ yr} \times \left( \frac{\alpha_{\text{GUT}}^{-1}}{25} \right)^2 \left( \frac{M_{\text{GUT}}}{10^{16} \text{ GeV}} \right)^4, \quad (36)$$

as

$$\tau(n' \rightarrow \nu' + a) \sim 3 \times 10^{19} \text{ s} \times \left( \frac{\tau_p}{10^{35} \text{ yr}} \right) \left( \frac{100 \text{ TeV}}{m_{N'}} \right)^5 \left( \frac{f_a}{100 \text{ TeV}} \right)^2 \left( \frac{10 \text{ TeV}}{f'_\pi} \right)^2. \quad (37)$$

Here  $\alpha_{\text{GUT}}$  denotes the fine-structure constant of the Grand Unified Theory. Thus, if the Hyper-Kamiokande experiment observes the proton decay with a lifetime of  $\mathcal{O}(10^{35})$  yr [90], the  $n'$  dark matter candidate is immediately excluded in combination with the EGRB observation in Eq. (35).

## ACKNOWLEDGEMENTS

The authors thank Cheng-Wei Chiang for useful discussions at the early stage of the project. This work is supported in part by Grants-in-Aid for Scientific Research from the Ministry of Education, Culture, Sports, Science, and Technology (MEXT) KAKENHI, Japan, No. 25105011 and No. 15H05889 (M. I.) as well as No. 26104009 (T. T. Y.); Grant-in-Aid No. 26287039 (M. I. and T. T. Y.) and No. 16H02176 (T. T. Y.) from the Japan Society for the Promotion of Science (JSPS) KAKENHI; and by the World Premier International Research Center Initiative (WPI), MEXT, Japan (M. I., and T. T. Y.). The work of H.F. is supported in part by a Research Fellowship for Young Scientists from the Japan Society for the Promotion of Science (JSPS).

## Appendix A: Explicit Breaking of the PQ-Symmetry

Throughout this paper, U(1) PQ-symmetry is assumed to be an almost exact symmetry of the model broken only by the axial anomaly. It is believed, however, that global symmetries are to be broken by Planck suppressed operators as generically expected in quantum gravity. For example, Planck suppressed self-interacting operators of  $\phi$

$$\mathcal{L}_{\mathcal{PQ}} = \frac{\kappa}{(n+4)!M_{\text{PL}}^n} (\phi^{n+4} + \phi^{*n+4}) , \quad (n > 0) , \quad (\text{A1})$$

with  $\kappa = O(1)$  break the PQ-symmetry explicitly. They lead to a non-vanishing effective  $\theta$ -angle at the minimum of the axion potential,

$$\Delta\theta_{\text{eff}} \sim \frac{\kappa}{2^{(n+2)/2}(n+3)!} \frac{f_a^{n+2}}{M_{\text{PL}}^n M_a^2} . \quad (\text{A2})$$

Thus, for dimension five operators ( $n = 1$ ), for example, the effective  $\theta$ -angle is given by

$$\Delta\theta_{\text{eff}} \sim 10^{-10} \times \kappa \left( \frac{f_a}{10^4 \text{ GeV}} \right)^3 \left( \frac{10 \text{ GeV}}{M_a} \right)^2 , \quad (\text{A3})$$

which is consistent with the current upper bound on the effective  $\theta$ -angle of  $\mathcal{O}(10^{-11})$  for  $f_a \lesssim O(10^3\text{--}10^4)$  and  $M_a = O(0.1\text{--}10) \text{ GeV}$ .<sup>17</sup>

In addition to the self-interacting operators in Eq. (A1), the other types of operators such as

$$\mathcal{L}_{\mathcal{PQ}} = \frac{|\Phi_{B-L}|^{2n}}{M_{\text{PL}}^{2n-3}} \phi + h.c. , \quad (\text{A4})$$

also leads to explicit breaking the PQ-symmetry. Here,  $\langle \Phi_{B-L} \rangle$  is the order parameter of the  $B - L$  symmetry. If we assume  $\langle \Phi_{B-L} \rangle \simeq 10^{10} \text{ GeV}$ , for example, the PQ-symmetry is badly broken for  $n = 2$ . To avoid this problem, it is required to assume that  $\phi$  has sizable couplings to the  $\psi^{(\prime)}$ , while it has highly suppressed couplings to the fields in the Standard Model sector and in the mirrored sector.

As another way to evade this problem, we may consider a model with an exact (and hence gauged) discrete symmetry under which  $\phi$  rotates non-trivially. For example, a model with a  $\mathbb{Z}_5$  discrete symmetry can be constructed by introducing five pairs of  $(\psi_L^{(\prime)}, \bar{\psi}_R^{(\prime)})$ . Under

<sup>17</sup> This feature is also advantageous to make a model where the PQ symmetry appears as an accidental symmetry resulting from other exact gauge symmetries (see [91, 92] and references therein).

the  $\mathbb{Z}_5$  symmetry,  $\phi$  has a charge  $-1$  while  $\psi_L$  and  $\psi'_L$  have the U(1) charge 0, and  $\bar{\psi}_R$  and  $\bar{\psi}'_R$  have the U(1) charge  $-1$ , with which the discrete symmetry is free from anomalies. In this model, the PQ-symmetry is realized an accidental symmetry while the PQ-breaking operators in Eq. (A4) is forbidden.

One problem of the model with an exact discrete symmetry is that the model causes the domain wall problem when it is spontaneously broken by  $\langle\phi\rangle$  [93, 94]. This problem can be avoided by assuming that  $\mathbb{Z}_5$  is embedded in a gauge U(1) symmetry so that U(1) symmetry is broken at a scale not very higher than  $f_a$ .<sup>18</sup> For example, we may consider a U(1) gauge symmetry under which  $\phi$  has a charge 1 while  $\psi_L$  and  $\psi'_L$  have a charge 0, and  $\bar{\psi}_R$  and  $\bar{\psi}'_R$  have a charge  $-1$ . Besides, we also introduce a scalar field  $X$  with a U(1) charge  $-5$  and pairs of colored left-handed Weyl fermions  $(\xi_L, \bar{\xi}_R)$  and  $(\xi'_L, \bar{\xi}'_R)$  with  $\xi_L^{(\prime)}$  and  $\bar{\xi}_R^{(\prime)}$  having the U(1) charges 3 and 2, respectively.<sup>19</sup> Under the U(1) gauge symmetry,  $\psi$ 's and  $\xi$ 's can couple via

$$\mathcal{L} = \phi\psi_L^{(\prime)}\bar{\psi}_R^{(\prime)} + X\xi_L^{(\prime)}\bar{\xi}_R^{(\prime)} + h.c. . \quad (\text{A5})$$

Then, once  $X$  obtains a VEV, the desired  $\mathbb{Z}_5$  symmetry remains with which the PQ-symmetry is realized as an approximate approximate symmetry. In this model, the domain wall is not stable and the domain wall problem can be evaded [95].

- 
- [1] R. D. Peccei and H. R. Quinn, Phys. Rev. Lett. **38**, 1440 (1977).
  - [2] R. D. Peccei and H. R. Quinn, Phys. Rev. **D16**, 1791 (1977).
  - [3] S. Weinberg, Phys. Rev. Lett. **40**, 223 (1978).
  - [4] F. Wilczek, Phys. Rev. Lett. **40**, 279 (1978).
  - [5] K. A. Olive *et al.* (Particle Data Group), Chin. Phys. **C38**, 090001 (2014).
  - [6] J. E. Kim, Phys. Rev. Lett. **43**, 103 (1979).
  - [7] M. A. Shifman, A. I. Vainshtein, and V. I. Zakharov, Nucl. Phys. **B166**, 493 (1980).
  - [8] A. R. Zhitnitsky, Sov. J. Nucl. Phys. **31**, 260 (1980), [Yad. Fiz.31,497(1980)].
  - [9] M. Dine, W. Fischler, and M. Srednicki, Phys. Lett. **B104**, 199 (1981).

<sup>18</sup> In such embedded models, the Peccei-Quinn breaking operators like Eq. A4 never appear due to the gauge symmetry. Thus, not  $\mathbb{Z}_5$  but  $\mathbb{Z}_4$  remnant symmetry may be sufficient.

<sup>19</sup> With this charge assignment, U(1) gauge symmetry is free from anomalies except for U(1)<sup>3</sup> anomaly. The U(1)<sup>3</sup> anomaly can be cancelled by introducing appropriate number of U(1) charged fermions which are neutral under the Standard Model<sup>(\prime)</sup> gauge symmetries.

- [10] S. Dimopoulos, Phys. Lett. **B84**, 435 (1979).
- [11] S. H. H. Tye, Phys. Rev. Lett. **47**, 1035 (1981).
- [12] V. A. Rubakov, JETP Lett. **65**, 621 (1997), arXiv:hep-ph/9703409 [hep-ph].
- [13] H. Fukuda, K. Harigaya, M. Ibe, and T. T. Yanagida, Phys. Rev. **D92**, 015021 (2015), arXiv:1504.06084 [hep-ph].
- [14] Z. Berezhiani, L. Gianfagna, and M. Giannotti, Phys. Lett. **B500**, 286 (2001), arXiv:hep-ph/0009290 [hep-ph].
- [15] A. Hook, Phys. Rev. Lett. **114**, 141801 (2015), arXiv:1411.3325 [hep-ph].
- [16] A. Albaid, M. Dine, and P. Draper, JHEP **12**, 046 (2015), arXiv:1510.03392 [hep-ph].
- [17] R. Barbieri, L. J. Hall, and K. Harigaya, JHEP **11**, 172 (2016), arXiv:1609.05589 [hep-ph].
- [18] S. W. Hawking, *Moscow Quantum Grav.1987:0125*, Phys. Lett. **B195**, 337 (1987).
- [19] G. V. Lavrelashvili, V. A. Rubakov, and P. G. Tinyakov, JETP Lett. **46**, 167 (1987), [Pisma Zh. Eksp. Teor. Fiz.46,134(1987)].
- [20] S. B. Giddings and A. Strominger, Nucl. Phys. **B307**, 854 (1988).
- [21] S. R. Coleman, Nucl. Phys. **B310**, 643 (1988).
- [22] G. Gilbert, Nucl. Phys. **B328**, 159 (1989).
- [23] T. Banks and N. Seiberg, Phys. Rev. **D83**, 084019 (2011), arXiv:1011.5120 [hep-th].
- [24] L. Ackerman, M. R. Buckley, S. M. Carroll, and M. Kamionkowski, Phys. Rev. **D79**, 023519 (2009), [,277(2008)], arXiv:0810.5126 [hep-ph].
- [25] J. L. Feng, M. Kaplinghat, H. Tu, and H.-B. Yu, JCAP **0907**, 004 (2009), arXiv:0905.3039 [hep-ph].
- [26] J. L. Feng, M. Kaplinghat, and H.-B. Yu, Phys. Rev. Lett. **104**, 151301 (2010), arXiv:0911.0422 [hep-ph].
- [27] P. Agrawal, F.-Y. Cyr-Racine, L. Randall, and J. Scholtz, (2016), arXiv:1610.04611 [hep-ph].
- [28] J. R. Ellis and M. K. Gaillard, Nucl. Phys. **B150**, 141 (1979).
- [29] C.-W. Chiang, H. Fukuda, M. Ibe, and T. T. Yanagida, Phys. Rev. **D93**, 095016 (2016), arXiv:1602.07909 [hep-ph].
- [30] F. Bergsma *et al.* (CHARM), Phys. Lett. **B157**, 458 (1985).
- [31] A. V. Artamonov *et al.* (BNL-E949), Phys. Rev. **D79**, 092004 (2009), arXiv:0903.0030 [hep-ex].
- [32] G. Aad *et al.* (ATLAS), JHEP **11**, 104 (2014), arXiv:1409.5500 [hep-ex].

- [33] G. Aad *et al.* (ATLAS), Phys. Rev. **D92**, 112007 (2015), arXiv:1509.04261 [hep-ex].
- [34] V. Khachatryan *et al.* (CMS), Phys. Rev. **D93**, 112009 (2016), arXiv:1507.07129 [hep-ex].
- [35] V. Khachatryan *et al.* (CMS), Phys. Rev. **D93**, 012003 (2016), arXiv:1509.04177 [hep-ex].
- [36] G. Aad *et al.* (ATLAS), JHEP **03**, 041 (2016), arXiv:1512.05910 [hep-ex].
- [37] H. Fukuda, M. Ibe, O. Jinnouchi, and M. Nojiri, (2016), arXiv:1607.01936 [hep-ph].
- [38] T. Yanagida, *Proceedings: Workshop on the Unified Theories and the Baryon Number in the Universe: Tsukuba, Japan, February 13-14, 1979*, Conf. Proc. **C7902131**, 95 (1979).
- [39] P. Ramond, in *International Symposium on Fundamentals of Quantum Theory and Quantum Field Theory Palm Coast, Florida, February 25-March 2, 1979* (1979) pp. 265–280, arXiv:hep-ph/9809459 [hep-ph].
- [40] P. Minkowski, Phys. Lett. **B67**, 421 (1977).
- [41] K. Osato, T. Sekiguchi, M. Shirasaki, A. Kamada, and N. Yoshida, JCAP **1606**, 004 (2016), arXiv:1601.07386 [astro-ph.CO].
- [42] M. Fukugita and T. Yanagida, Phys. Lett. **B174**, 45 (1986).
- [43] G. F. Giudice, A. Notari, M. Raidal, A. Riotto, and A. Strumia, Nucl. Phys. **B685**, 89 (2004), arXiv:hep-ph/0310123 [hep-ph].
- [44] W. Buchmuller, R. D. Peccei, and T. Yanagida, Ann. Rev. Nucl. Part. Sci. **55**, 311 (2005), arXiv:hep-ph/0502169 [hep-ph].
- [45] S. Davidson, E. Nardi, and Y. Nir, Phys. Rept. **466**, 105 (2008), arXiv:0802.2962 [hep-ph].
- [46] P. H. Frampton, S. L. Glashow, and T. Yanagida, Phys. Lett. **B548**, 119 (2002), arXiv:hep-ph/0208157 [hep-ph].
- [47] M. Raidal and A. Strumia, Phys. Lett. **B553**, 72 (2003), arXiv:hep-ph/0210021 [hep-ph].
- [48] A. Ibarra and G. G. Ross, Phys. Lett. **B591**, 285 (2004), arXiv:hep-ph/0312138 [hep-ph].
- [49] K. Harigaya, M. Ibe, and T. T. Yanagida, Phys. Rev. **D86**, 013002 (2012), arXiv:1205.2198 [hep-ph].
- [50] C. Patrignani *et al.* (Particle Data Group), Chin. Phys. **C40**, 100001 (2016).
- [51] A. Walker-Loud, *Proceedings, 31st International Symposium on Lattice Field Theory (Lattice 2013): Mainz, Germany, July 29-August 3, 2013*, PoS **LATTICE2013**, 013 (2014), arXiv:1401.8259 [hep-lat].
- [52] P. A. R. Ade *et al.* (Planck), (2015), arXiv:1502.02114 [astro-ph.CO].
- [53] P. Gondolo and G. Gelmini, Nucl. Phys. **B360**, 145 (1991).



- [54] G. Steigman, B. Dasgupta, and J. F. Beacom, Phys. Rev. **D86**, 023506 (2012), arXiv:1204.3622 [hep-ph].
- [55] K. Griest and M. Kamionkowski, Phys. Rev. Lett. **64**, 615 (1990).
- [56] S. Weinberg, Phys. Rev. Lett. **17**, 616 (1966).
- [57] J. Kang, M. A. Luty, and S. Nasri, JHEP **09**, 086 (2008), arXiv:hep-ph/0611322 [hep-ph].
- [58] K. Harigaya, M. Ibe, K. Kaneta, W. Nakano, and M. Suzuki, (2016), arXiv:1606.00159 [hep-ph].
- [59] B. von Harling and K. Petraki, JCAP **1412**, 033 (2014), arXiv:1407.7874 [hep-ph].
- [60] K. Petraki, M. Postma, and M. Wiechers, JHEP **06**, 128 (2015), arXiv:1505.00109 [hep-ph].
- [61] H. An, M. B. Wise, and Y. Zhang, Phys. Rev. **D93**, 115020 (2016), arXiv:1604.01776 [hep-ph].
- [62] K. Petraki, M. Postma, and J. de Vries, (2016), arXiv:1611.01394 [hep-ph].
- [63] J. A. Adams, S. Sarkar, and D. W. Sciama, Mon. Not. Roy. Astron. Soc. **301**, 210 (1998), arXiv:astro-ph/9805108 [astro-ph].
- [64] X.-L. Chen and M. Kamionkowski, Phys. Rev. **D70**, 043502 (2004), arXiv:astro-ph/0310473 [astro-ph].
- [65] T. R. Slatyer, N. Padmanabhan, and D. P. Finkbeiner, Phys. Rev. **D80**, 043526 (2009), arXiv:0906.1197 [astro-ph.CO].
- [66] T. Kanzaki, M. Kawasaki, and K. Nakayama, Prog. Theor. Phys. **123**, 853 (2010), arXiv:0907.3985 [astro-ph.CO].
- [67] S. Galli, F. Iocco, G. Bertone, and A. Melchiorri, Phys. Rev. **D80**, 023505 (2009), arXiv:0905.0003 [astro-ph.CO].
- [68] M. Kawasaki, K. Nakayama, and T. Sekiguchi, Phys. Lett. **B756**, 212 (2016), arXiv:1512.08015 [astro-ph.CO].
- [69] T. R. Slatyer, Phys. Rev. **D93**, 023527 (2016), arXiv:1506.03811 [hep-ph].
- [70] J. M. Cline and P. Scott, JCAP **1303**, 044 (2013), [Erratum: JCAP1305,E01(2013)], arXiv:1301.5908 [astro-ph.CO].
- [71] H. Liu, T. R. Slatyer, and J. Zavala, Phys. Rev. **D94**, 063507 (2016), arXiv:1604.02457 [astro-ph.CO].
- [72] T. Bringmann, F. Kahlhoefer, K. Schmidt-Hoberg, and P. Walia, (2016), arXiv:1612.00845 [hep-ph].
- [73] P. A. R. Ade *et al.* (Planck), Astron. Astrophys. **594**, A13 (2016), arXiv:1502.01589 [astro-

- ph.CO].
- [74] D. A. Buote, T. E. Jeltema, C. R. Canizares, and G. P. Garmire, *Astrophys. J.* **577**, 183 (2002), arXiv:astro-ph/0205469 [astro-ph].
  - [75] F. Kahlhoefer, K. Schmidt-Hoberg, M. T. Frandsen, and S. Sarkar, *Mon. Not. Roy. Astron. Soc.* **437**, 2865 (2014), arXiv:1308.3419 [astro-ph.CO].
  - [76] M. Kaplinghat, S. Tulin, and H.-B. Yu, *Phys. Rev. Lett.* **116**, 041302 (2016), arXiv:1508.03339 [astro-ph.CO].
  - [77] G. Mangano, G. Miele, S. Pastor, T. Pinto, O. Pisanti, and P. D. Serpico, *Nucl. Phys.* **B729**, 221 (2005), arXiv:hep-ph/0506164 [hep-ph].
  - [78] B. W. Lee and S. Weinberg, *Phys. Rev. Lett.* **39**, 165 (1977).
  - [79] A. Kogut *et al.*, *JCAP* **1107**, 025 (2011), arXiv:1105.2044 [astro-ph.CO].
  - [80] T. Matsumura *et al.*, (2013), 10.1007/s10909-013-0996-1, [*J. Low. Temp. Phys.*176,733(2014)], arXiv:1311.2847 [astro-ph.IM].
  - [81] C. J. A. P. Martins, in *Proceedings, 50th Rencontres de Moriond Gravitation : 100 years after GR: La Thuile, Italy, March 21-28, 2015* (2015) pp. 185–188.
  - [82] G. Giesen, M. Boudaud, Y. Génolini, V. Poulin, M. Cirelli, P. Salati, and P. D. Serpico, *JCAP* **1509**, 023 (2015), arXiv:1504.04276 [astro-ph.HE].
  - [83] M. Ibe, S. Matsumoto, S. Shirai, and T. T. Yanagida, *Phys. Rev.* **D91**, 111701 (2015), arXiv:1504.05554 [hep-ph].
  - [84] Ams-02 Collaboration, Talks at the ‘AMS Days at CERN’ (15-17 april 2015).
  - [85] M. Ackermann *et al.* (Fermi-LAT), *Phys. Rev. Lett.* **115**, 231301 (2015), arXiv:1503.02641 [astro-ph.HE].
  - [86] A. Ibarra and D. Tran, *Phys. Rev. Lett.* **100**, 061301 (2008), arXiv:0709.4593 [astro-ph].
  - [87] K. Ishiwata, S. Matsumoto, and T. Moroi, *Phys. Lett.* **B679**, 1 (2009), arXiv:0905.4593 [astro-ph.CO].
  - [88] E. Carquin, M. A. Diaz, G. A. Gomez-Vargas, B. Panes, and N. Viaux, *Phys. Dark Univ.* **11**, 1 (2016), arXiv:1501.05932 [hep-ph].
  - [89] S. Ando and K. Ishiwata, *JCAP* **1505**, 024 (2015), arXiv:1502.02007 [astro-ph.CO]; *JCAP* **1606**, 045 (2016), arXiv:1604.02263 [hep-ph].
  - [90] Hyper-Kamiokande Design Report (2016).
  - [91] K. Harigaya, M. Ibe, K. Schmitz, and T. T. Yanagida, *Phys. Rev.* **D88**, 075022 (2013),

- arXiv:1308.1227 [hep-ph].
- [92] M. Redi and R. Sato, *JHEP* **05**, 104 (2016), arXiv:1602.05427 [hep-ph].
- [93] Ya. B. Zeldovich, I. Yu. Kobzarev, and L. B. Okun, *Zh. Eksp. Teor. Fiz.* **67**, 3 (1974), [*Sov. Phys. JETP*40,1(1974)].
- [94] T. W. B. Kibble, *J. Phys.* **A9**, 1387 (1976).
- [95] H. Fukuda, M. Ibe, M. Suzuki, and T. T. Yanagida, In preparation.